Vegetally localised Vrtn functions as a novel repressor to modulate bmp2b transcription during dorsoventral patterning in zebrafish

Ming Shao, Min Wang, Yuan-Yuan Liu, Yi-Wen Ge, Yan-Jun Zhang, De-Li Shi

HAL Id: hal-04004478

https://hal.sorbonne-universite.fr/hal-04004478v1

Submitted on 6 Mar 2023

Vegetally localised Vrtn functions as a novel repressor to modulate *bmp2b* transcription during dorsoventral patterning in zebrafish

Ming Shao[1], Min Wang[1], Yuan-Yuan Liu[1], Yi-Wen Ge[1], Yan-Jun Zhang[1] and De-Li Shi[1,2,*]

ABSTRACT

The vegetal pole cytoplasm represents a crucial source of maternal dorsal determinants for patterning the dorsoventral axis of the early embryo. Removal of the vegetal yolk in the zebrafish fertilised egg before the completion of the first cleavage results in embryonic ventralisation, but removal of this part at the two-cell stage leads to embryonic dorsalisation. How this is achieved remains unknown. Here, we report a novel mode of maternal regulation of BMP signalling during dorsoventral patterning in zebrafish. We identify Vrtn as a novel vegetally localised maternal factor with dorsalising activity and rapid transport towards the animal pole region after fertilisation. Co-injection of *vrtn* mRNA with vegetal RNAs from different cleavage stages suggests the presence of putative vegetally localised Vrtn antagonists with slower animal pole transport. Thus, vegetal ablation at the two-cell stage could remove most of the Vrtn antagonists, and allows Vrtn to produce the dorsalising effect. Mechanistically, Vrtn binds a *bmp2b* regulatory sequence and acts as a repressor to inhibit its zygotic transcription. Analysis of maternal-zygotic *vrtn* mutants further shows that Vrtn is required to constrain excessive *bmp2b* expression in the margin. Our work unveils a novel maternal mechanism regulating zygotic BMP gradient in dorsoventral patterning.

KEY WORDS: Bmp2b, BMP signalling, Dorsoventral patterning, Vegetal maternal determinants, Vrtn, Zebrafish

INTRODUCTION

The formation of dorsoventral (DV) axis is one of the earliest developmental processes that establishes the animal body plan. The dorsal determinants (DDs) model suggests an intimate relationship between animal-vegetal polarity and the DV axis, because dorsalising signals are enriched in the vegetal pole of the oocyte. Triggered by fertilisation and controlled by microtubules, DDs are asymmetrically transported, from vegetal pole to the prospective dorsal side in zebrafish (Abrams and Mullins, 2009; Mei et al., 2009; Nojima et al., 2010; Langdon and Mullins, 2011; Shao et al., 2012; Tran et al., 2012; Ge et al., 2014) and in *Xenopus* (Cuykendall and Houston, 2009; Slack, 2014; Carron and Shi, 2016). Several candidate DDs, including Dishevelled, GBP, and Wnt11 in *Xenopus* (Miller et al., 1999; Weaver et al., 2003; Tao et al., 2005), and Wnt8a in zebrafish (Lu et al., 2011), were thought to be required for dorsal axis formation. In zebrafish, DDs activate Wnt/β-catenin signalling in the dorsal region of the blastula, causing the stabilisation and nuclear localisation of β-catenin 2, which is essential for zygotic expression of dorsal organiser genes (Bellipanni et al., 2006). One of the pivotal pieces of evidence supporting the DDs model is the vegetal pole ablation (VAb) experiment. Removing vegetal yolk cell before the first cleavage reduces or blocks the activation of maternal Wnt/β-catenin signalling and results in ventralisation. This suggests that DDs first localise at the vegetal pole in the oocyte, and rapidly evacuate this region soon after fertilisation (Mizuno et al., 1999; Ober and Schulte-Merker, 1999). Consistent with this model, several vegetally localised factors, including syntabulin (Nojima et al., 2010) and Grip2a (Ge et al., 2014), have been shown to be involved in the dorsal transportation of DDs.

Bone morphogenetic proteins (BMPs), mainly zygotically supplied in zebrafish, are key factors required for ventral fate specification. Several studies have suggested that Bmp genes initiate their zygotic transcription under the control of maternal factors. Gdf6a activates zygotic Bmp gene expression through its receptors Alk6 and/or Alk8 (Goutel et al., 2000; Sidi et al., 2003). In dorsalised maternal-zygotic (MZ) *spg* (MZ*spg*) or maternal (M) *spg* (M*spg*) embryos, in which *pou5f3* is mutated, the transcription of Bmp genes is inhibited (Reim and Brand, 2006). Moreover, the maternal factors MGA, Max and Smad4 act in the yolk syncytial layer (YSL) to maintain *bmp2b* expression, and initiate a positive-feedback loop of BMP signalling within the embryo (Sun et al., 2014). Thus, these factors are required for zygotic expression of Bmp genes in the lateral and ventral regions. In the dorsal region, however, initial zygotic *bmp2b* transcription is suppressed by a DD-mediated pathway (Leung et al., 2003). Weak expression then appears in the shield, which helps to generate a correct BMP activity gradient along the DV axis (Xue et al., 2014). In *Xenopus*, the presence of BMP signalling in the Spemann organiser has been proposed as a mechanism that ensures the self-regulation of the morphogenetic field (Dosch and Niehrs, 2000; Reversade et al., 2005; De Robertis, 2006; Inui et al., 2012). These results suggest that dorsal transcription of Bmp genes is tightly regulated to adjust the activity of the organiser and pattern the DV axis. However, how the early transcription of Bmp genes in other regions of the embryo is regulated remains largely elusive.

The zygotic transcription of Bmp genes in the lateral and ventral regions of the zebrafish embryo is activated by different maternal factors (Goutel et al., 2000; Sidi et al., 2003; Reim and Brand, 2006). There are also clues for the presence of repressive factors that function independently of DDs to modulate their expression. In particular, VAb after the two-cell stage can produce unexpected dorsalisation (Mizuno et al., 1999). These embryos display a general decrease of *bmp2b* expression, which is not accompanied by an increase of Wnt/β-catenin signalling. This is intriguing, but how it is achieved remains unclear. In this study, we investigated the mechanism underlying this novel mode of maternal regulation of

[1]School of Life Science, Shandong University, 27 Shanda Nan road, Jinan 250100, China. [2]Sorbonne Universités, UPMC Univ Paris 06, CNRS UMR7622, IBPS-Developmental Biology Laboratory, 75005 Paris, France.

*Author for correspondence (de-li.shi@upmc.fr)

D.-L.S., 0000-0002-6104-9137

bmp2b expression. We find that the dorsalisation caused by VAb after the two-cell stage occurs in the absence of the dorsal organiser, and is specifically associated with a disrupted zygotic *bmp2b* expression pattern and a reduced BMP activity. Mechanistically, we identified and characterised Vrtn (vertebrae development associated) as a novel vegetally localised transcriptional repressor. It is rapidly transported to the animal pole region after fertilisation and binds to a *bmp2b* regulatory region to prevent its transcription. This work uncovers a novel antagonist or repressor of embryonic ventralisation, which functions independently of, but in cooperation with, Wnt/β-catenin signalling to regulate DV patterning.

RESULTS

VAb after the two-cell stage causes dorsalisation independently of Wnt/β-catenin signalling

In order to understand how VAb after the two-cell stage causes dorsalisation, the effects were re-evaluated during early development. We found that VAb-mediated dorsalisation was stage dependent. VAb between the two- and 16-cell stages (VAb@2cell) produced a high proportion of dorsalised embryos (Fig. S1A,B), which displayed enlarged dorsal tissues at the expense of ventral fate. Some embryos showed the highest degree of dorsalisation (C5) (Kishimoto et al., 1997), with radial neural marker expression, expanded paraxial tissues and absence of lateral tissues such as the prospective pronephric duct, as revealed by the expression pattern of *pax2.1*, *egr2b* (*krox20*) and *myod1* (Fig. S1C-E′). By contrast, VAb before the two-cell stage (VAb@1cell) mainly caused ventralisation. The embryos showed increased pronephric precursor cells, and reduced or absent paraxial and axial tissues (Fig. S1F-G′).

The dorsalised phenotype could be caused by activation of dorsalising signals, such as maternal Wnt/β-catenin, or by inhibition of ventralising signals, such as BMP and zygotic Wnt/β-catenin. An inhibition of zygotic Wnt/β-catenin never produces a characteristic long and elliptical phenotype at 12 hours post-fertilisation (hpf), which is reminiscent of BMP-deficient embryos (Ramel et al., 2005). To determine if VAb@2cell-induced dorsalisation was due to activation of maternal Wnt/β-catenin signalling, we examined target genes of this pathway, *goosecoid* (*gsc*), *dharma*/*bozozok* (*dha*/*boz*) and *chordin* (*chd*), at sphere or 50% epiboly stage by *in situ* hybridisation. Compared with intact embryos, the expression of these genes was either normal or reduced (Fig. S2A-I). Consistently, the nuclear localisation of endogenous β-catenin at 3.5 hpf was unchanged or reduced (Fig. S2J-L), excluding the possibility that VAb@2cell triggers activation of Wnt/β-catenin signalling.

Cell non-autonomous inhibition of BMP signalling in VAb@2cell embryos

To test whether VAb@2cell causes BMP inhibition, we first examined P-Smad1/5/8 level. Compared with intact embryos, a large majority of VAb@2cell embryos at 60% epiboly showed no or weak P-Smad1/5/8 immunostaining (Fig. 1A,B). Using western blotting, we also detected a 42% decrease of P-Smad1/5/8 level in VAb@2cell embryos at 70% epiboly, compared with a 20.6% increase in VAb@1cell embryos at the same stage (Fig. 1C,D). We then examined the BMP target genes *eve1* and *gata2a*. The expression of *eve1* was reduced in a majority of VAb@2cell embryos at 50% epiboly (Fig. 1E), suggesting BMP inhibition. When the expression patterns of *gata2a* and *gsc* were simultaneously examined at 70% epiboly, we found that 60% of VAb@2cell embryos (*n*=15) showed reduced *gata2a* expression, but with varied *gsc* expression patterns. Notably, *gata2a* expression was inhibited in some VAb@2cell embryos with absence of *gsc*
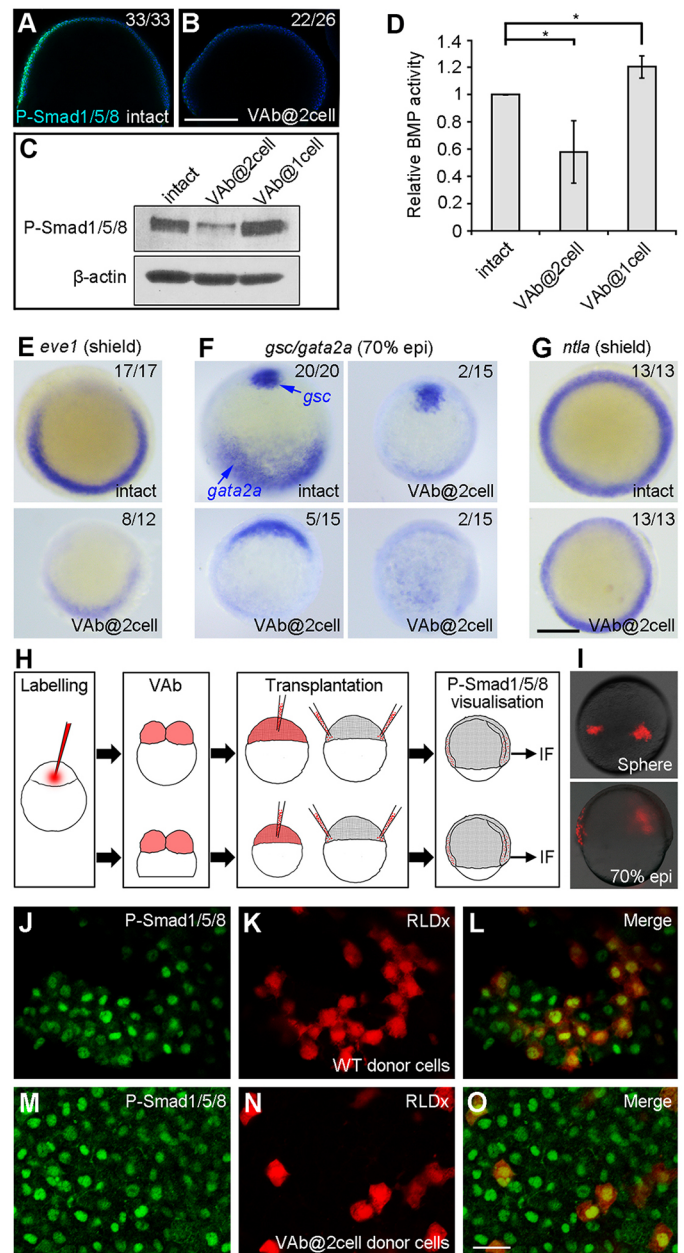

Fig. 1. VAb@2cell inhibits BMP signalling. (A,B) Decreased P-Smad1/5/8 immunostaining (green), merged with DAPI (blue), in VAb@2cell embryos at 60% epiboly. (C,D) Analysis by western blotting of P-Smad1/5/8 levels in VAb@2cell and VAb@1cell embryos at 70% epiboly. P-Smad1/5/8 levels are normalised to β-actin, and BMP activity in intact embryos is set as 1. Data are mean±s.d. from three independent experiments. (E-G) Analysis by *in situ* hybridisation of indicated genes. Animal pole views with dorsal at the top. (H) Procedure of cell transplantation to visualise cell non-autonomous inhibition of BMP signalling in VAb@2cell embryos using P-Smad1/5/8 immunofluorescence (IF) staining. (I) RLDx-labelled donor cells transplanted at different locations of the margin in unlabelled intact embryos at 70% epiboly. (J-O) Similar presence of P-Smad1/5/8 immunostaining in transplanted cells derived from intact (J-L) or VAb@2cell (M-O) embryos. Scale bars: 250 μm in A,B,E-G; 20 μm in J-O.

expression (Fig. 1F). In all examined VAb@2cell embryos (13/13), *ntla* expression was unaffected (Fig. 1G). These results suggest that BMP inhibition after VAb@2cell is independent of the dorsal organiser. Thus, there may be maternal factors inhibiting BMP activity in the lateral and ventral regions.

We next performed transplantation experiments to examine how cells from VAb@2cell embryos interpret endogenous BMP signal. At sphere stage, deep blastoderm cells from RLDx-labelled VAb@2cell embryos were transplanted to two separate positions within the margin of unlabelled normal recipients to increase the probability of their ventral location (Fig. 1H,I). At 70% epiboly, P-Smad1/5/8 was similarly detected by immunostaining in transplanted cells from control and VAb@2cell embryos (Fig. 1J-O). Furthermore, when differentially labelled cells from intact and VAb@2cell embryos were mixed and transplanted to the ventral margin of unlabelled recipients, they colocalised in posterior muscle, epidermis and blood at 24 hpf (Fig. S3). These indicate that cells in VAb@2cell embryos were able to receive and activate BMP signal, and could normally undergo differentiation. Accordingly, injection of *bmp2b* mRNA (25 pg) in VAb@2cell embryos efficiently prevented dorsalisation (Fig. S4). As BMP signalling in these embryos is inhibited in a cell non-autonomous manner, VAb@2cell should not block BMP transduction downstream of extracellular ligands.

VAb@2cell inhibits zygotic *bmp2b* expression

One possibility is that VAb@2cell causes a deficiency of BMP ligands. In zebrafish, three Bmp genes, *bmp2b*, *bmp7a* and *bmp4*, initiate their expression after mid-blastula transition, and maintain a DV gradient transcription during late blastula and gastrula stages. Both Bmp2b and Bmp7a are essential for DV patterning, but only the Bmp2b/Bmp7a heterodimer is capable of activating the BMP pathway (Little and Mullins, 2009). Consistently, loss of either *bmp2b* or *bmp7a* causes severe dorsalisation (Kishimoto et al., 1997; Schmid et al., 2000; Dick et al., 2000), whereas loss of *bmp4* affects ventral fate only in posterior tissues (Stickney et al., 2007). We thus examined by *in situ* hybridisation the expression of these Bmp genes in VAb@2cell embryos. Zygotic transcription of *bmp7a* and its expression in the early gastrula were unaffected (Fig. 2A-D). The expression of *bmp4* was also unchanged in the early gastrula (Fig. 2E,F), although it was not maintained at mid-gastrula stage (Fig. 2G,H), but this alone cannot account for the severely dorsalised phenotype. As for *bmp2b*, the initiation of its zygotic transcription was unaffected (Fig. 2I,J); however, the marginal upregulation from late blastula to early gastrula stages was strongly reduced (Fig. 2K,L,O). At 75% epiboly (mid-gastrula), *bmp2b* expression in intact embryos was restricted to the ventral ectoderm in a relatively homogeneous pattern, whereas it became scattered in the ventral half in more than half of VAb@2cell embryos (Fig. 2M-N′). Moreover, *bmp2b* expression was localised in
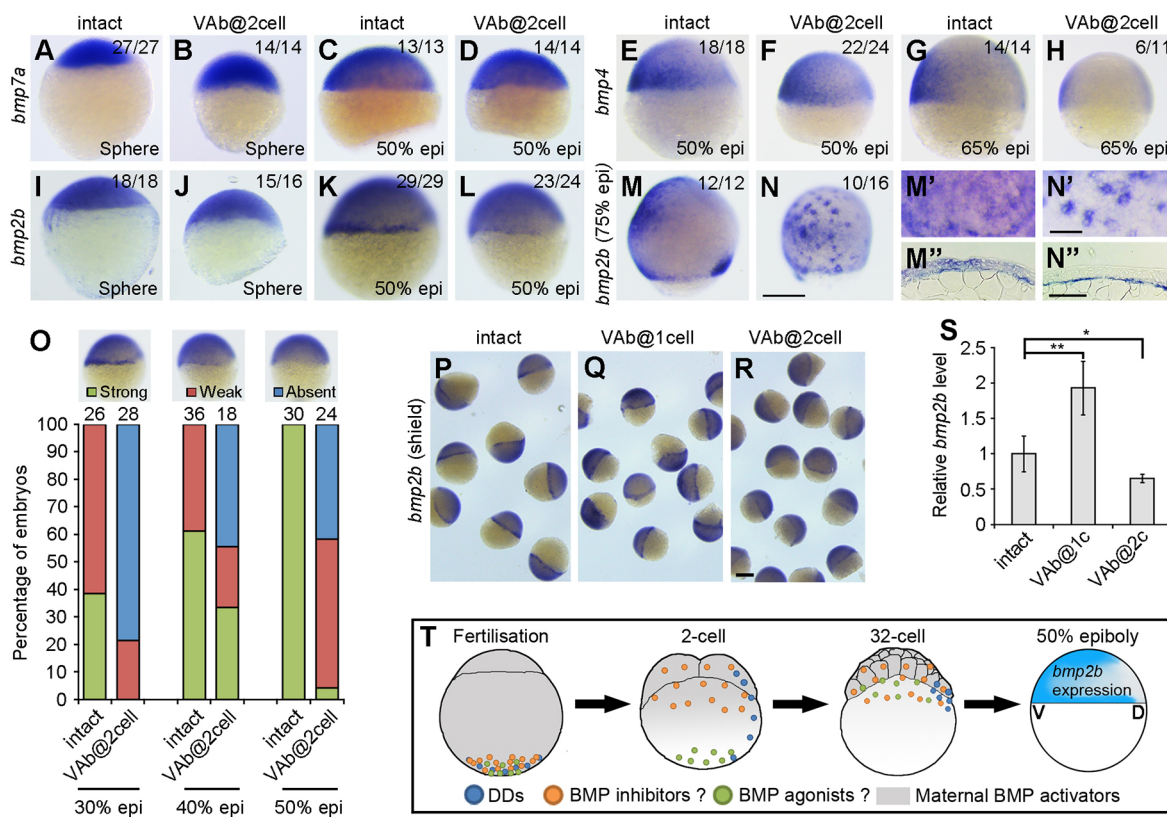

Fig. 2. Differential expression of Bmp genes in VAb@2cell embryos. (A-D) Similar expression pattern of *bmp7a* in intact and VAb@2cell embryos at the indicated stages. (E-H) The expression pattern of *bmp4* remains unchanged in VAb@2cell embryos at 50% epiboly, but is strongly reduced at 65% epiboly. (I-L) The initiation of *bmp2b* expression is unaffected in VAb@2cell embryos at sphere-dome stage, but its zygotic transcription in the margin is reduced or absent at 50% epiboly. (M,N) Scattered *bmp2b* expression pattern in VAb@2cell embryos at 75% epiboly. Lateral views with dorsal on the right. (M′,N′) Higher magnification in the ventral-animal region of indicated embryos. (M″,N″) Localisation of *bmp2b* in indicated embryos. (O) Statistical analysis of *bmp2b* marginal expression in intact and VAb@2cell embryos at the indicated stages, with representative images shown at the top. Numbers on the top of the graph indicate total embryos from two independent experiments. (P-R) Comparison of *bmp2b* expression in indicated embryos at 50% epiboly. The *bmp2b* marginal expression is maintained or enhanced in VAb@1cell embryos, but is suppressed in VAb@2cell embryos. (S) Analysis by qRT-PCR of *bmp2b* levels in VAb@1cell and VAb@2cell embryos. Data are mean±s.d. from four independent experiments. (T) A working hypothesis to explain the dorsalising effect of VAb@2cell. In addition to DDs, putative BMP inhibitors and agonists are also vegetally localised. After fertilisation, the BMP inhibitors should be transported to the animal pole region more rapidly than the BMP agonists; this may account for the appearance of the dorsalised phenotype after VAb@2cell. Scale bars: 250 μm in A-N,P-R; 100 μm in M′-N″.

blastoderm cells of intact embryos, whereas it became restricted in the internal YSL (I-YSL) of VAb@2cell embryos (Fig. 2M″,N″). Furthermore, in contrast to VAb@2cell embryos, *bmp2b* expression in VAb@1cell embryos was enhanced at 50% epiboly (Fig. 2P-S). These indicate that VAb@2cell specifically inhibits *bmp2b* transcription in the margin.

To further test whether blocking *bmp2b* marginal expression mimics the dorsalising effect of VAb@2cell, we specifically inhibited *bmp2b* in the margin by injecting translation-blocking morpholino (*bmp2b*MO) into the yolk at 128-cell stage (Fig. S5A-C). The result showed that almost half of the injected embryos (n=45) were severely dorsalised (C4-C5). However, when *bmp2b*MO was injected into the YSL at 512-cell stage, nearly all embryos developed normally (Fig. S5D,E). Collectively, these results suggest the presence of vegetally localised maternal BMP inhibitors, which should have been transported to the blastoderm margin as early as at the two-cell stage at a comparable speed as the vegetally localised DDs (Jesuthasan and Strähle, 1997). There may also be BMP agonists that counteract the activity of the BMP inhibitors. However, they should display a relatively slow animal pole transport after fertilisation (Fig. 2T). Thus, when VAb is performed at the two-cell stage, most of the BMP agonists are removed. The animal pole-transported BMP inhibitors could repress *bmp2b* transcription, and may be responsible for the dorsalising effect of VAb@2cell. By contrast, VAb@1cell removes DDs, the BMP inhibitors and the BMP agonists, and the presence of maternal BMP activators results in ventralisation.

Identification of Vrtn as a novel vegetally localised BMP inhibitor

In order to verify the above hypothesis, we aimed to identify potential vegetally localised BMP regulators. The transcripts for *dazl*, *celf1* and *mago nashi* (*magoh*) were shown to be vegetally

localised (Maegawa et al., 1999; Suzuki et al., 2000; Marlow and Mullins, 2008), but their overexpression did not produce any effect (Fig. S6). This suggests that they should not function as a BMP regulator. We thus sought to identify other factors responsible for the dorsalising and BMP-inhibiting activity in VAb@2cell embryos. Animal and vegetal pole regions from fertilised eggs were dissected and subjected to high-throughput RNA-seq (Fig. 3A). Besides a number of known factors, we uncovered *vrtn* as a novel vegetally enriched transcript (Table S1). The cDNA encodes an uncharacterised polypeptide that does not belong to any known protein family. In pigs, this gene is possibly associated with variation in vertebral number (Mikawa et al., 2011), but its function in early development is totally obscure.

The RNA-seq data were further confirmed by *in situ* hybridisation during oogenesis and early development. In stage I oocyte, *vrtn* transcripts were detected in the ooplasm, with evident enrichment in the Balbiani body (Fig. S7A,B). They were gradually localised in the vegetal cortex at late stages of oogenesis (Fig. S7C-F). This vegetal localisation was particularly evident in fertilised eggs (Fig. 3B). However, as early as at the two-cell stage, *vrtn* transcripts began to be deposited as punctate forms at the blastodisc margin (Fig. 3C,D), suggesting a rapid transport. As the yolk cell cortex at the two-cell stage is thin and large, the hybridisation signal may not properly reflect the amount of migrating *vrtn* transcripts. At 50% epiboly, *vrtn* transcripts were restricted to the entire margin and YSL (Fig. 3E,F). During gastrulation, they were maintained in the ventral margin but were downregulated in the dorsal and animal pole regions (Fig. 3G). As development proceeds, *vrtn* expression shifted to the neural plate boundary and newly formed somites at the one-somite stage (Fig. 3H,I), and was restricted in the tail-bud region at the six-somite stage (Fig. 3J). We then performed VAb at different stages to examine how this removes *vrtn* transcripts. *In situ* hybridisation at the 32-cell stage showed that VAb@1cell strongly reduced the marginal
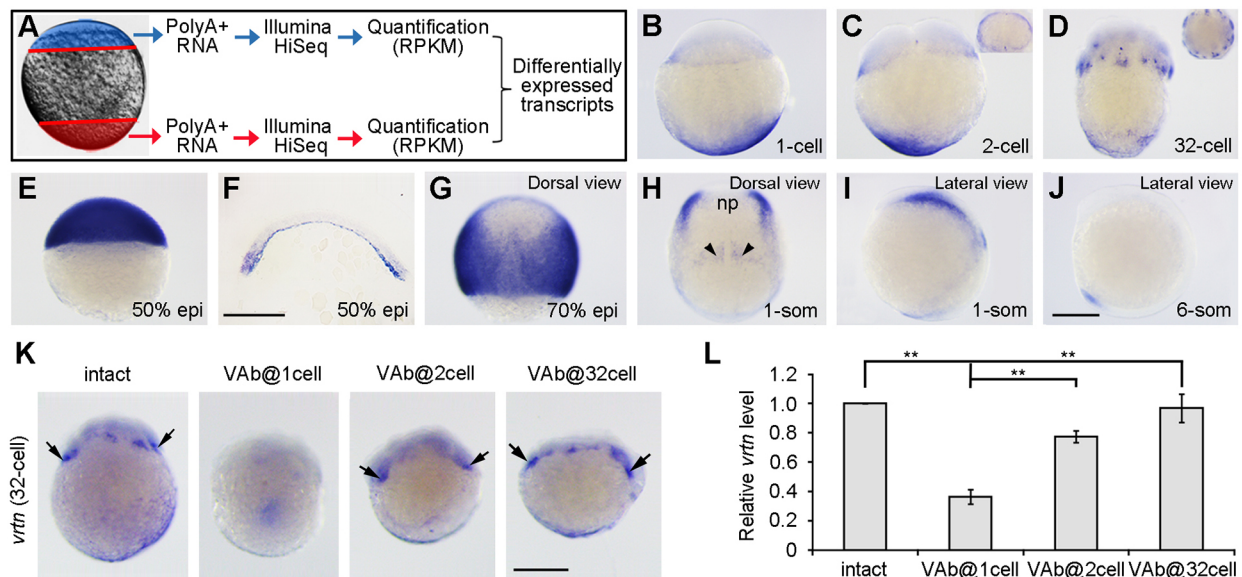

Fig. 3. Identification of vegetally localised *vrtn* transcripts. (A) Procedure for the identification of vegetal pole-enriched transcripts. (B) Maternal *vrtn* transcripts are localised to the vegetal pole region in the fertilised egg. (C) At the two-cell stage, *vrtn* transcripts are detected in the marginal region. The inset is an animal pole view. (D) At the 32-cell stage, most *vrtn* transcripts are localised in the marginal region, as shown by the animal pole view (inset). (E) Strong *vrtn* expression in the blastoderm at 50% epiboly. (F) Vertical section showing marginal and YSL expression of *vrtn* at 50% epiboly. (G) Dorsal view at 70% epiboly shows strong *vrtn* expression in the lateral region. (H,I) Dorsal and lateral views show *vrtn* expression in the neural plate boundary (np) and forming somites (arrowheads) at the one-somite stage. (J) Lateral view shows *vrtn* expression in the tail-bud at the six-somite stage. (K) Analysis by *in situ* hybridisation of *vrtn* expression following VAb at indicated stages. Arrows indicate the marginal accumulation of maternal *vrtn* transcripts. (L) Analysis by qRT-PCR of *vrtn* levels. The relative *vrtn* level in intact embryos is normalised as 1; data are mean±s.d. from three independent experiments. Scale bars: 250 μm.

accumulation of *vrtn* transcripts, whereas VAb at the 2-cell stage had no or weak effect (Fig. 3K). Analysis by qRT-PCR indicated that more than 60% of *vrtn* transcripts were removed after VAb@1cell, compared with a 20% reduction after VAb@2cell, and an absence of effect after VAb@32cell (Fig. 3L). Collectively, these observations reveal the vegetal localisation and rapid transport of maternal *vrtn* transcripts.

To determine whether Vrtn functions as a BMP regulator in DV patterning, we performed overexpression by injecting synthetic *vrtn* mRNA (100 pg) and found that this caused varied degrees of dorsalisation, depending on the time of injection (Fig. 4A,B, Fig. S8). We then examined the expression patterns of *dha/boz* and *gsc*, and found that they were unaffected at the sphere stage (Fig. 4C-E), indicating that the dorsalising effect of Vrtn was independent of maternal Wnt/β-catenin signalling. However, as in VAb@2cell embryos, *gata2a* expression was inhibited in 35% of *vrtn*-injected embryos (*n*=17), whereas *gsc* expression was not obviously expanded at 70% epiboly (Fig. 4C,F). Consistently, P-Smad1/5/8 level was reduced in 50% of *vrtn*-injected embryos (*n*=10) at 75% epiboly, and *bmp2b* marginal expression was suppressed in 60% of *vrtn*-injected embryos (*n*=35) at 50% epiboly (Fig. 4C,G). Moreover, as in VAb@2cell embryos, 54% of *vrtn*-injected

embryos (*n*=13) at 70% epiboly showed a scattered *bmp2b* expression pattern (Fig. 4C). These results strongly suggest that Vrtn overexpression mimics the effect of VAb@2cell. We further asked whether Vrtn could synergise with the dorsalising effect of VAb@2cell. Embryos at the one-cell stage were injected with a low amount of *vrtn* mRNA (30 pg), and a fraction of these embryos was subjected to VAb@2cell. Intact embryos injected with *vrtn* and uninjected VAb@2cell embryos displayed 5.4% and 9.5% severely dorsalised phenotype (C4-C5), respectively. However, *vrtn*-injected VAb@2cell embryos exhibited 22.2% severely dorsalised phenotype, along with a significant increase of other less-dorsalised phenotypes (Fig. 4H). This clearly indicates a synergistic effect between Vrtn and VAb@2cell.

To test whether Vrtn regulates BMP pathway activation, we examined its effect on Bmp2b-induced ventralisation and target gene expression. Co-injection of *vrtn* mRNA (300 pg) with *bmp2b* mRNA (100 pg) did not modify Bmp2b-ventralised phenotype (Fig. S9A-E), and failed to prevent Bmp2b-induced upregulation of *eve1* and *gata2a* (Fig. S9F,G). Thus, in this experimental condition, Vrtn does not block signal transduction by Bmp2b.
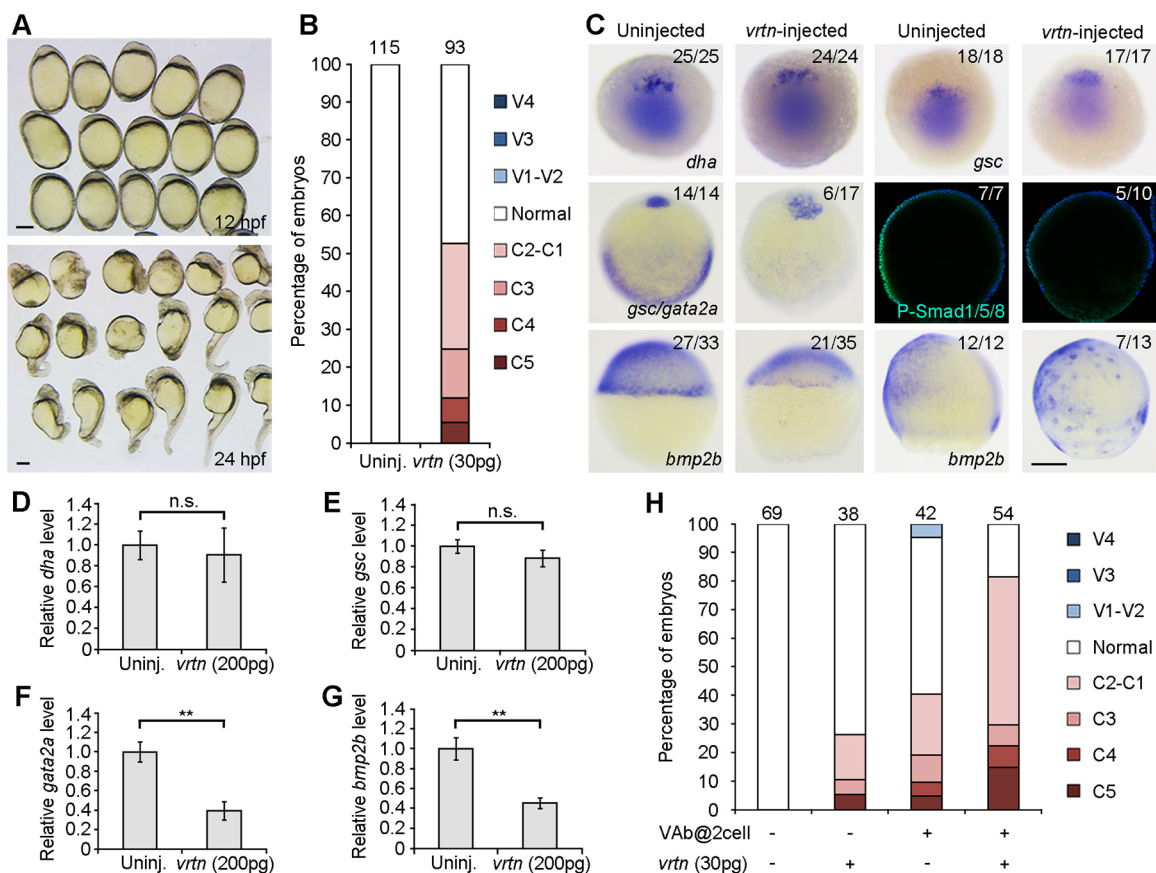

Fig. 4. Vrtn overexpression produces dorsalisation and suppresses BMP signalling. (A) Dorsalised embryos at 12 and 24 hpf following Vrtn overexpression. (B) Statistical analysis of Vrtn-dorsalised embryos at 24 hpf. Numbers at the top indicate the total embryos from three independent experiments. (C) Early effects of Vrtn overexpression. The expression patterns of *dha/boz* and *gsc* remain unchanged at the sphere stage, and *gata2a* expression at 70% epiboly and P-Smad1/5/8 level at 60% epiboly are suppressed. The marginal transcription of *bmp2b* is inhibited at 50% epiboly, and scattered I-YSL expression of *bmp2b* is present at 70% epibloy. (D-G) Analysis by qRT-PCR of the expression level of *dha/boz*, *gsc*, *gata2a* and *bmp2b* in Vrtn-overexpressing embryos. The relative expression level in uninjected embryos is normalised as 1; data are mean values±s.d. from four independent experiments. (H) Statistical analysis of the synergistic effect between VAb@2cell and Vrtn overexpression. Numbers at the top indicate the total number of embryos from two independent experiments. Scale bars: 250 µm.

VAb@2cell-mediated dorsalisation is suppressed in MZvrtn mutants

We next used CRISPR/Cas9 to generate *vrtn* mutants. A 10 bp nucleotide deletion was obtained in the second exon. This produces a frameshift in the 5′ region of the coding sequence and a premature stop codon, which presumably results in a truncated peptide with the first 17 amino acids (Fig. 5A). In particular, the mutation led to nonsense-mediated decay. In MZ*vrtn* mutants, *vrtn* transcripts were absent, especially in the vegetal pole region, although zygotic transcripts were detected at a much lower level (Fig. S10A-D). Analysis by qRT-PCR revealed a 95.6% decrease of the mutant transcripts at cleavage stages, and a 90.7% decrease at shield stage (Fig. S10E). Along with a rigorous allele-specific PCR analysis (Fig. S10F), it can be concluded that we have generated a loss-of-function mutation of *vrtn* gene.

The M*vrtn* and MZ*vrtn* embryos displayed a mildly ventralised phenotype (V1) with a small head at 27 hpf (Fig. 5B). To exclude the possibility that the reduced head size may be caused by a developmental delay of mutant embryos, we first visualised eye field and forebrain regions at bud stage by *in situ* hybridisation using *rx3* and *six3b*, respectively, and found reduced expression domains of these genes in M*vrtn* and MZ*vrtn* mutants (Fig. 5C). We further labelled nine-somite stage embryos with *six3b* and *myod1*, and measured head length and the *six3b* expression domain. The results showed that the head size was significantly reduced in M*vrtn* and MZ*vrtn* mutants, compared with wild-type (WT) embryos with an equal number of somites. Moreover, M*vrtn* and MZ*vrtn* embryos displayed the same phenotype (Fig. 5D-F), indicating that the lack of maternal *vrtn* is sufficient to generate the ventralised phenotype. Furthermore, both *in situ* hybridisation and qRT-PCR analyses indicated that *gsc* and *dha*/*boz* expression was unaffected at mid-blastula stage (Fig. 5G,H), but *bmp2b* expression was enhanced at 50% epiboly (Fig. 5I), and *otx2* expression domain was reduced at 80% epiboly (Fig. 5J). We then injected translation-blocking *vrtn* morpholino (*vrtn*MO) into wild-type embryos to see whether knockdown of *vrtn* affects DV patterning. Although *vrtn*MO efficiently blocked the translation of an artificial mRNA where the *vrtn*MO-targeting sequence was fused to *vrtn*-GFP (Fig. S11A-D), it did not produce a ventralised phenotype (Fig. S11E,F). Those *vrtn* morphants showed a reduction of somite number at 36 hpf (Fig. S11G,H), as in MZ*vrtn* mutants (Fig. S11I). The absence of effect following *vrtn* knockdown may be due to the presence of maternal Vrtn protein. Further analysis will be necessary to determine whether the induction of a compensatory mechanism is responsible for the mild MZ*vrtn* mutant phenotype.

To analyse whether the dorsalising effect of VAb@2cell depends on Vrtn activity, we performed VAb@2cell in MZ*vrtn* embryos. In sharp contrast to wild-type embryos, VAb@2cell in MZ*vrtn* embryos had almost no dorsalising effect (Fig. 5K). Intriguingly, they displayed essentially ventralised phenotypes (Fig. 5L), with strongly increased *bmp2b* expression at shield stage, as revealed by *in situ* hybridisation and qRT-PCR (Fig. 5M, N). This suggests that MZ*vrtn* embryos are extremely sensitive to the reduction in DDs. To directly test this possibility, we injected β-catenin 2 morpholino (*β-cat2*MO) into wild-type and MZ*vrtn* embryos to compare the ventralising effect. As reported (Bellipanni et al., 2006), most *β-cat2*MO-injected wild-type embryos exhibited mildly ventralised phenotype. However, there was a strong increase in the severely ventralised phenotype in *β-cat2*MO-injected MZ*vrtn* embryos (Fig. S12). This implies that DDs and Vrtn functionally interact and cooperate to control the BMP morphogenetic field.

With respect to the dorsalising effect of VAb@2cell in wild-type embryos, the mildly ventralised MZ*vrtn* mutant phenotype may be interpreted by the presence of other vegetal factors that are transported slowly to the animal pole and function to counteract the activity of Vrtn. To test this possibility, we extracted vegetal RNAs at the two- to four-cell stages in MZ*vrtn* embryos, which avoids the interference by endogenous Vrtn protein, and co-injected with *vrtn* mRNA (250 pg) in wild-type embryos. Using P-Smad1/5/8 as a readout, we found a 60% decrease of BMP activity in *vrtn*-injected embryos at 50% epiboly, and a significant rescue by vegetal RNAs, which did not affect BMP activity when injected alone (Fig. 6A,B). To examine how Vrtn activity may be temporally regulated by the putative vegetal factors, we assayed the activity of vegetal RNAs from MZ*vrtn* embryos at different stages to antagonise Vrtn function. We found that only four-cell stage vegetal RNAs robustly restored Vrtn-inhibited P-Smad1/5/8 levels (Fig. 6C,D) and efficiently alleviated the Vrtn-dorsalised phenotype (Fig. 6E,F). These observations establish that Vrtn represents a novel vegetally localised factor and functions as a repressor of embryonic ventralisation by inhibiting zygotic *bmp2b* transcription. They also suggest that Vrtn activity might be antagonised by other vegetal factors with different kinetics of animal pole transport.

Vrtn acts as a transcriptional repressor

To further understand how Vrtn functions, its subcellular localisation in zebrafish and mammalian cells was analysed by immunostaining and live imaging. Consistent with previous observations (Mikawa et al., 2011), myc- or GFP-tagged zebrafish Vrtn was enriched in the nucleus during interphase of the cell cycle (Fig. 7A-E, Fig. S13), but was released to the cytoplasm in M-phase cells (Fig. S13, Movie 1). As no functional domain and no classical nuclear localisation signal (NLS) could be predicted on the protein, we aligned 47 Vrtn sequences from 45 species and identified five conserved domains, designated as CD1 to CD5 (Fig. S14). These domains were individually deleted and overexpressed by injecting the corresponding mRNA (100 pg). The results showed that deletion of CD1 or CD3 severely disrupted Vrtn nuclear targeting (Fig. S15), suggesting that potential non-classical NLS that are recognised by non-classical nuclear transport receptors may be present in these domains.

We then used the *UAS*-Gal4 one-hybrid system to investigate how Vrtn functions as a transcriptional regulator (Fig. 7F). Different synthetic mRNAs (100 pg) encoding full-length or truncated Vrtn proteins fused to Gal4 were co-injected with a luciferase reporter driven by the *5×UAS* and a minimal *hsp70* promoter in zebrafish embryos (Fig. 7G). Gal4-Vrtn suppressed the reporter activity by almost 90%, in a similar manner to Gal4-ENR, a known transcriptional repressor, whereas Gal4 or Vrtn alone had no effect (Fig. 7H). Gal4-Vrtn could not alter the activity of *xbra-luc*, an unrelated reporter (Fig. 7I). Moreover, Gal4-Vrtn eliminated GFP expression under the control of *UAS* elements, but had no effect on GFP transcription driven by *EF1α* promoter (Fig. 7J-M). These demonstrate that Vrtn functions to repress gene transcription. We then examined Vrtn functional domains involved in the repressor activity, and found that Gal4-dCD1 suppressed less than 30% of the luciferase activity, whereas Gal4-dCD2 showed a weak decrease of repressive activity (Fig. 7N,O). However, Gal4-dCD3, Gal4-dCD4 and Gal4-dCD5 retained a similar repressive activity to Gal4-Vrtn (Fig. 7N,O). These indicate that Vrtn acts as a potent transcriptional repressor, and that its N-terminal domains are crucial for the repressor function.
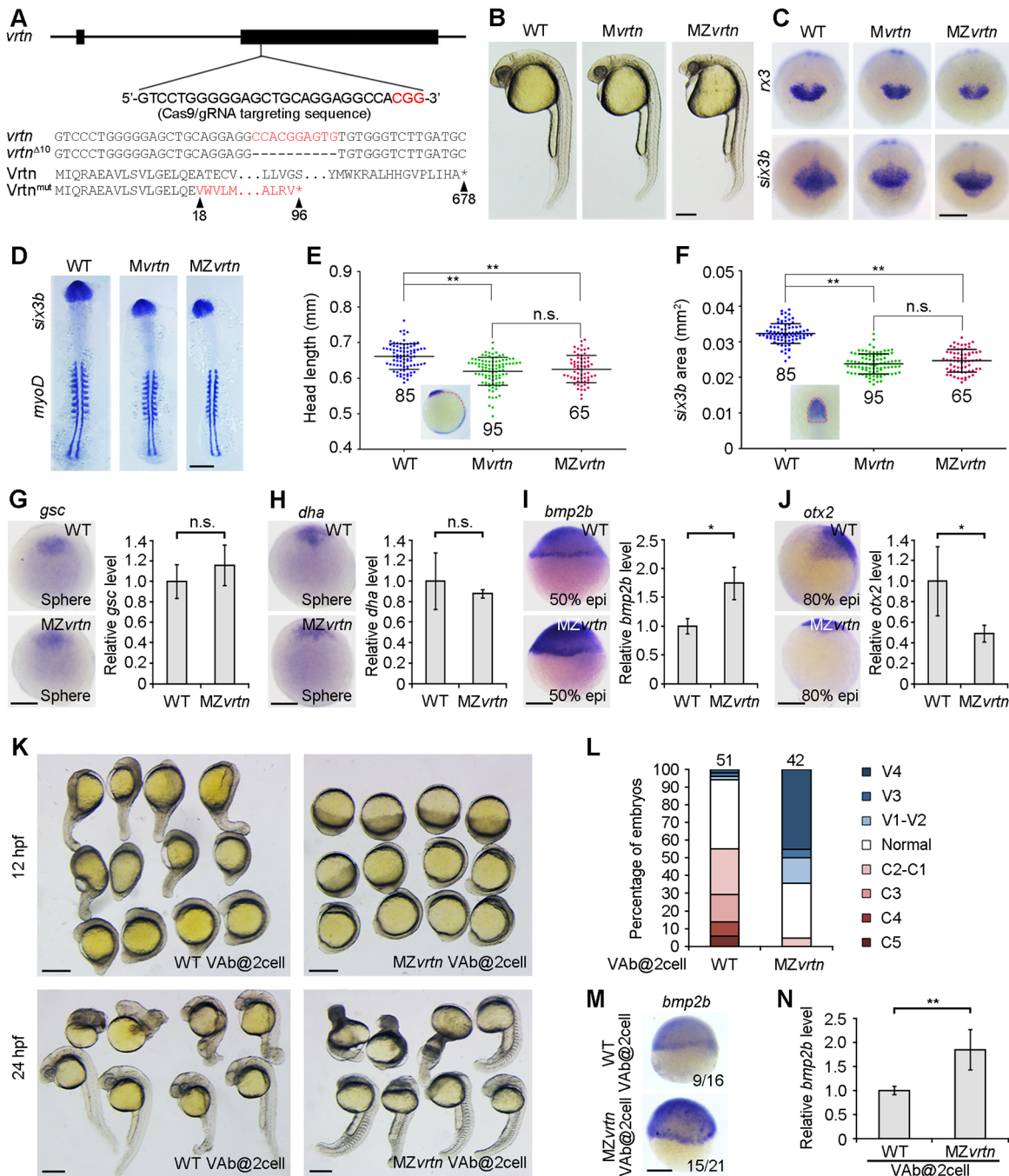
Fig. 5. The dorsalising effect of VAb@2cell is suppressed in MZ*vrtn* mutants. (A) Targeted mutation of the *vrtn* gene. The Cas9/gRNA targeting sequence and the PAM region (red) are shown, and the mutated allele with the predicted peptide is indicated. (B) Representative images of indicated embryos at 27 hpf, showing smaller eyes and reduced head size in *vrtn* mutants. (C) Decreased *rx3* and *six3b* expression domains in *vrtn* mutants at the bud stage. (D) Expression patterns of *six3b* and *myod1* in flat-mounted embryos with equal somite numbers. (E,F) Analysis by scatter plots of head length and *six3b* expression area at the six-somite stage. The red broken lines in the insets define the parameters of measurement. Horizontal lines represent the mean±s.d. from three batches of embryos with the total number indicated. (G-J) Analyses by *in situ* hybridisation and qRT-PCR of the expression of *gsc*, *dha/boz*, *bmp2b* and *otx2* in MZ*vrtn* mutants. The expression of *gsc* and *dha/boz* remains unchanged at sphere stage (animal pole views), the expression of *bmp2b* is enhanced at 50% epiboly, and the expression of *otx2* is reduced at 80% epiboly (lateral views with dorsal on the right). The relative expression level in wild-type embryos is normalised as 1; data are mean±s.d. from three independent experiments. (K) MZ*vrtn* embryos are ventralised following VAb@2cell. (L) Statistical analysis of the ventralising effect. Numbers at the top represent total embryos from three independent experiments. (M,N) Analyses by *in situ* hybridisation and qRT-PCR of *bmp2b* expression at the shield stage in wild-type and MZ*vrtn* embryos after VAb@2cell. The embryos are shown as lateral views. The relative *bmp2b* level in VAb@2cell wild-type embryos is set as 1; data are mean±s.d. from six independent experiments. Scale bars: 250 µm.

Vrtn binds a *bmp2b* upstream sequence and represses its transcription

We next investigated whether Vrtn binds DNA to function as a transcription factor. This was achieved first by chromatin

immunoprecipitation (ChIP). Zebrafish embryos were injected with synthetic *vrtn*-myc mRNA (100 pg) at the one-cell stage and crosslinked at 50% epiboly. The sonicated chromatins were precipitated with anti-myc antibody. Analyses by PCR and qPCR
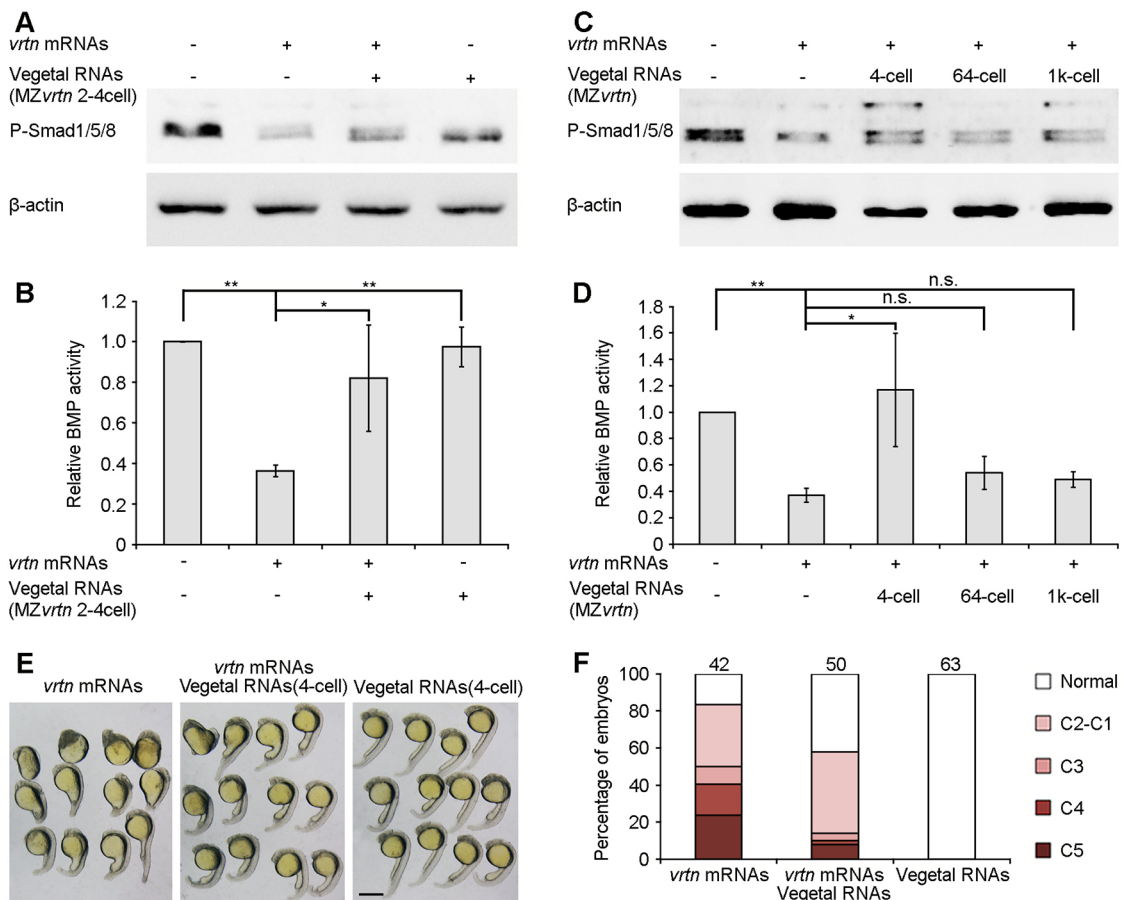
Fig. 6. Vegetal RNAs antagonise the dorsalising and BMP-inhibiting activity of Vrtn. (A) Western blotting at 50% epiboly shows the rescue of P-Smad1/5/8 levels in Vrtn-overexpressing embryos by vegetal RNAs from the two- to four-cell stage. (B) P-Smad1/5/8 level is normalised to β-actin and quantified with respect to uninjected embryos. Data are mean±s.d. from four independent experiments. (C) Western blotting shows the temporal regulation of Vrtn activity by vegetal RNAs. (D) Quantification of P-Smad1/5/8 level. Vegetal RNAs from 64- or 1000-cell stages show no effect on Vrtn-inhibited P-Smad1/5/8 levels. Data are mean±s.d. from three independent experiments. (E,F) Representative embryos at 24 hpf and statistical analysis show that vegetal RNAs counterbalance Vrtn-mediated dorsalisation. Numbers at the top indicate total embryos from two independent experiments. Scale bar: 200 μm.

showed that a −4775 to −4664 bp amplicon upstream of the transcription start site of the *bmp2b* locus was significantly enriched by Vrtn-myc (Fig. 8A-F). To test whether this region represents a functional silencer of *bmp2b*, a −5701 to −3772 fragment and a −800 to +605 fragment were fused to luciferase reporter. A control reporter contained the −800 to +605 region (Fig. 8G). Synthetic *vrtn* mRNA (500 pg) was co-injected with these reporters at the one-cell stage, and luciferase activity was assayed at 50% epiboly. We found that Vrtn suppressed by about threefold the luciferase activity driven by the −5701 to −3772 fragment, but it had no effect on the control reporter (Fig. 8H,I). Eletrophoretic mobility shift assays (EMSAs) were then employed to determine the binding sequence. Myc-tagged Vrtn was expressed in zebrafish embryos for preparation of Vrtn-containing nuclear lysates, and five *bmp2b* probes (p1-p5) located within and outside the ChIP-enriched region were labelled with biotin (Fig. 8J, Table S3). The analyses indicated that only the p2 probe encompassing the −4775 to −4716 region upstream of the transcription start site resulted in a specific high molecular weight band shift, which was competed for by an excess of unlabelled p2 probe. Other probes did not show a shift of the same size (Fig. 8K,L). These results clearly suggest that Vrtn possesses the ability to bind the *bmp2b* regulatory sequence directly. Taken together, our results suggest that Vrtn interacts with the *bmp2b* regulatory sequence to repress its transcription.

DISCUSSION

We show that zebrafish Vrtn is a novel vegetally localised regulator of *bmp2b* transcription in DV patterning. Maternal *vrtn* transcripts start to transport towards the animal pole immediately after fertilisation and co-localise with *bmp2b* in the margin after the onset of zygotic transcription. Vrtn binds the *bmp2b* upstream regulatory region and represses its zygotic transcription independently of Wnt/β-catenin signalling. These findings identify a novel maternal mechanism that ensures a correct BMP gradient for DV axis formation.

Early studies in amphibians have established that the Spemann organiser expresses both BMP signalling antagonists and BMP ligands, which is required for establishing a correct BMP gradient (Carron and Shi, 2016), and represents a mechanism of self-regulation of the morphogenetic field (Reversade et al., 2005; De Robertis, 2006). Thus, both the expression, including the initial transcription and late maintenance, and the activity of BMP ligands in the dorsal region are tightly regulated by either a positive or a negative mechanism. There are different kinds of evidence indicating that BMP activity in the ventral region is controlled by similar mechanisms. In zebrafish, *bmp2b*, *bmp7a* and *bmp4* are expressed in the lateral and ventral regions during late blastula and gastrula stages. Several maternal factors, including Gdf6a and Pou5f3, were shown to play a crucial role for initiating their zygotic
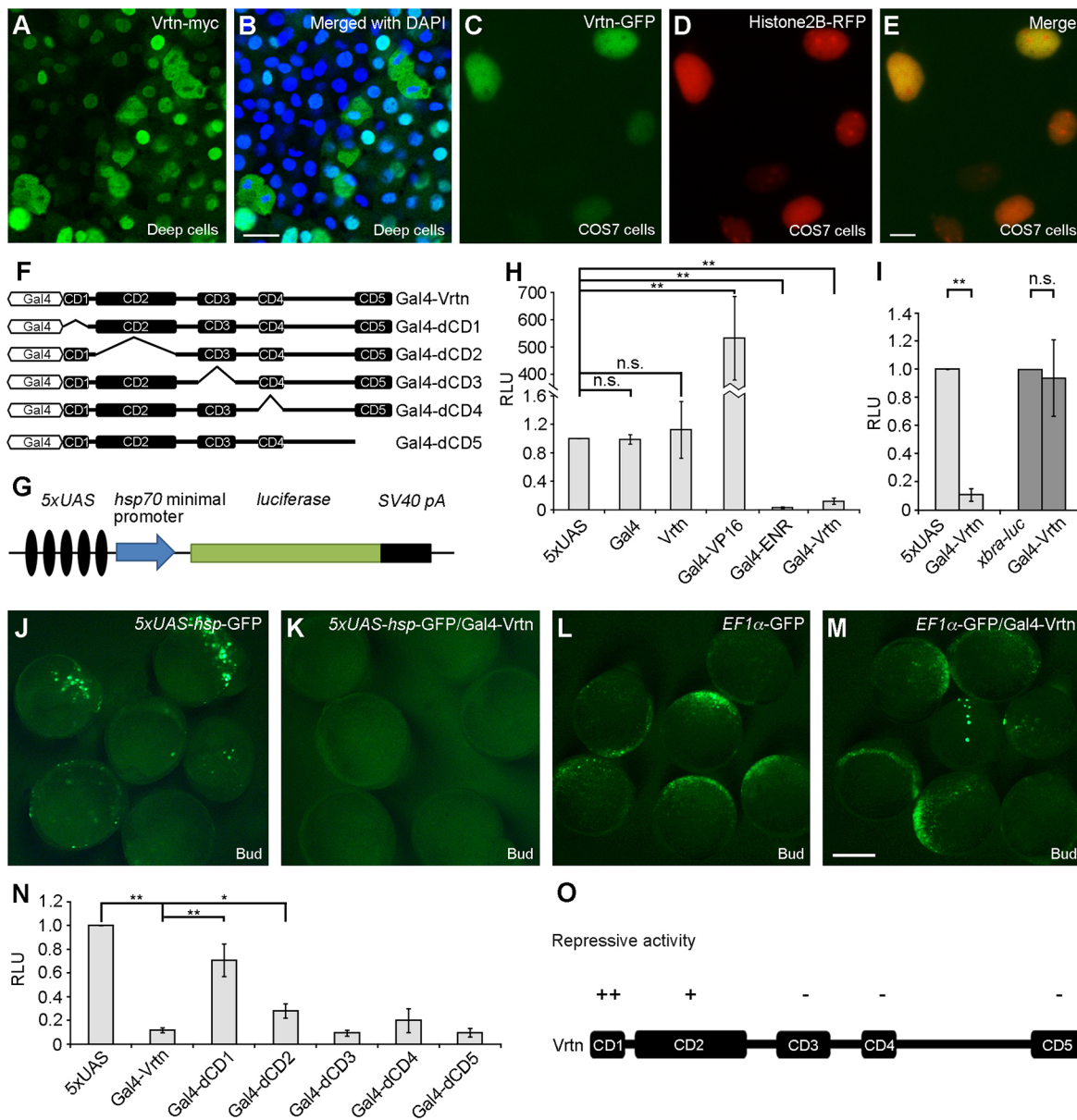
Fig. 7. Vrtn functions as a transcriptional repressor. (A,B) Nuclear localisation of Vrtn-myc in deep cells of zebrafish embryos at 50% epiboly. (C-E) Nuclear localisation of Vrtn-GFP in COS7 cells. (F) Schematic of full-length and truncated Vrtn fused with a Gal4 DNA-binding domain. (G) Schematic shows the *5×UAS-hsp-luc* reporter. (H) Graph shows the specificity and validity of the one-hybrid assay system. Data are mean±s.d. from three independent experiments. (I) Gal4-Vrtn has no effect on the *xbra* promoter. Data are mean±s.d. from three independent experiments. (J-M) Gal4-Vrtn suppresses GFP transcription driven by the *5×UAS-hsp* promoter, but not by the *EF1α* promoter. The embryos were injected with *5×UAS-hsp-GFP* plasmid (100 pg) or *EF1α-GFP* plasmid (20 pg), either alone or together with *Gal4-Vrtn* mRNA (200 pg). (N) Graph shows the transcriptional repressor activity of full-length and truncated Vrtn. Data are mean±s.d. from three independent experiments. (O) Summary of the repressive activity of Vrtn domains. Scale bars: 20 μm in A,B; 10 μm in C-E; 200 μm in J-M.

transcription (Sidi et al., 2003; Reim and Brand, 2006). However, it is unclear whether there are maternal factors preventing their excessive upregulation before the formation of the dorsal organiser. In the present study, we uncovered Vrtn as a maternal factor representing one of the possible mechanisms limiting BMP activation. In particular, we find that Vrtn-induced dorsalisation is achieved by transcriptional repression of zygotic *bmp2b* expression in the lateral and ventral margins of the late blastula.

The downregulation of *bmp2b* by Vrtn is not caused by the positive autoregulation of BMP pathway. In *swr* or *snh* mutants with loss-of-function of *bmp2b* or *bmp7a*, respectively, BMP signalling is blocked due to the absence of functional Bmp2b/Bmp7a heterodimer and *bmp2b*-positive auto-regulation. However, in

each mutant, *bmp2b* expression is only strongly reduced at mid- to late-gastrula stages, but is almost normal at shield stage (Nguyen et al., 1998; Hild et al., 1999; Kondo, 2007). This indicates that the *bmp2b* positive-feedback loop is established after shield stage, much later than the initiation of its marginal upregulation at 30% epiboly. Furthermore, *vrtn* overexpression abolishes *bmp2b* expression only in the ventral ectoderm at mid-gastrula stage, leaving relatively intact or enhanced expression in the I-YSL, whereas in *swr* or *snh* mutant, *bmp2b* expression shows an overall reduction, both in the ectoderm and I-YSL (Nguyen et al., 1998). These suggest that the marginal upregulation of *bmp2b* transcription should not be controlled by the positive-feedback loop of BMP signalling. It is likely activated by maternal factors such as Gdf6a
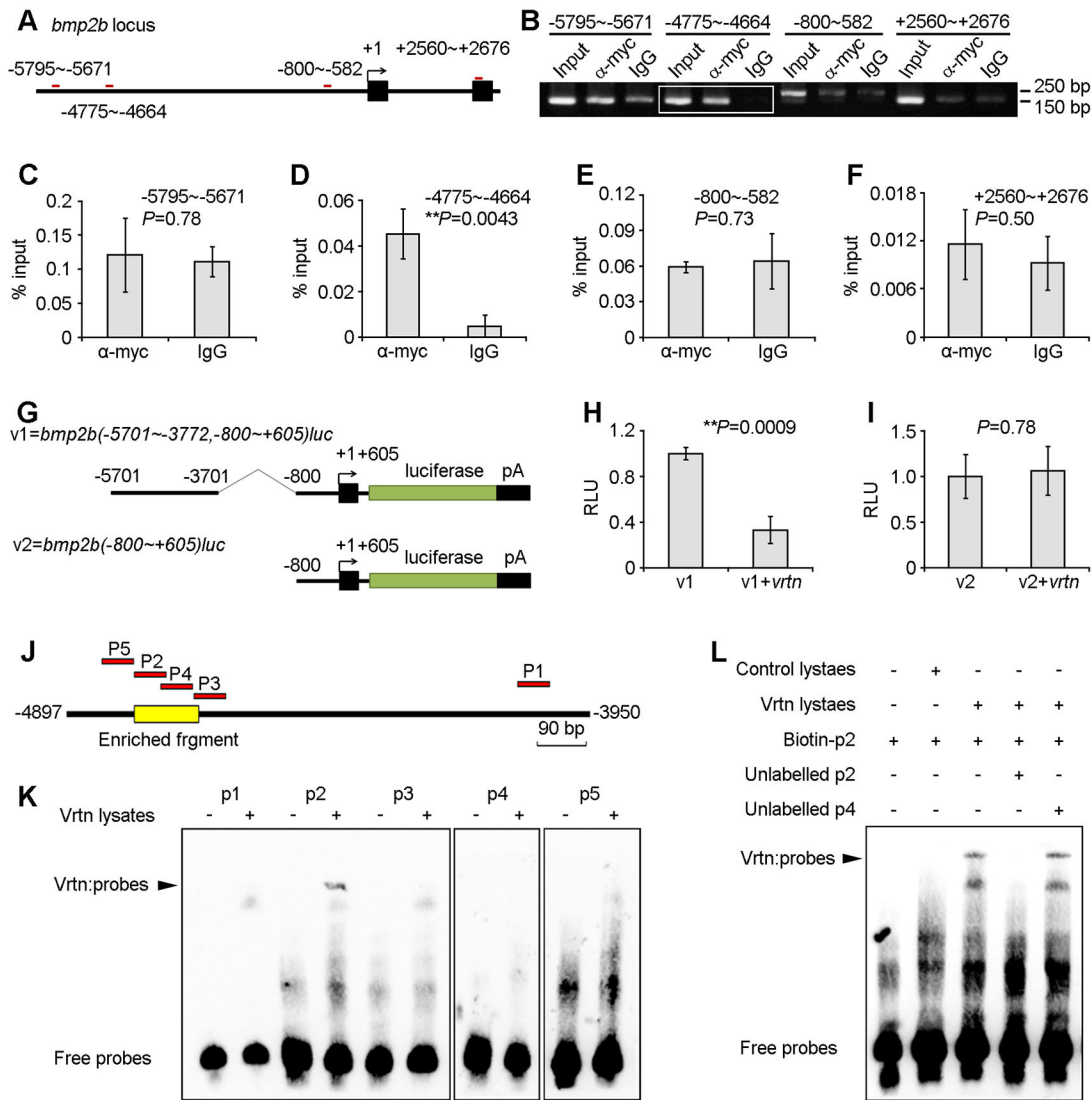
Fig. 8. Vrtn binds *bmp2b* upstream sequence and suppresses its transcription. ChIP (A-F) and EMSA (J-L) were performed using zebrafish embryos overexpressing myc-tagged Vrtn. (A) Schematic shows the location of different amplicons (red lines) in the *bmp2b* locus. (B) A representative ChIP-PCR result shows the specific enrichment of the −4775 to −4664 fragment (boxed). (C-F) Analysis by qPCR of different amplicons. Bars represent the mean values±s.d. from three independent experiments. (G) Representation of *bmp2b* luciferase reporters. (H,I) Vrtn represses v1, but not v2, *bmp2b* reporter activity. Data are mean±s.d. from three independent experiments. (J) Schematic shows the position of the EMSA probes in *bmp2b* locus. (K) Band shift assay. Vrtn forms a high-mobility complex with p2 probe (arrowhead). (L) Competition of Vrtn binding to biotin-labelled p2 by an excess of unlabelled p2, but not by p4. Two independent experiments were performed with the same result.

and Pou5f3 (Sidi et al., 2003; Reim and Brand, 2006), whereas Vrtn plays an inhibitory role to limit this upregulation.

The mechanism by which Vrtn functions in DV axis formation is also different from other maternal factors. The marginal transcription of *bmp2b* at shield stage is intact in *runx2bt2* morphants, and in MZ*p18ahub* (*ints6*) and MZ*split top* (*ctsba*) mutants (Flores et al., 2008; Kapp et al., 2013; Langdon et al., 2016). Loss of function of these genes, as well as *lnx2b* (Ro and Dawid, 2009), leads to an early expansion of dorsal organiser gene expression, often associated with a downregulation of *ved* and *vox*, and/or reduced zygotic Wnt/β-catenin signalling. The detailed molecular mechanisms by which these genes regulate DV axis formation are not known, except for Lnx2b, which is an E3 ubiquitin ligase that negatively regulates Dha/Boz function through the ubiquitin proteasome pathway (Ro and Dawid, 2009). Nevertheless, the above phenotypes are obviously different from those that result from VAb@2cell and Vrtn

overexpression, which do not cause a reduction of zygotic Wnt/β-catenin activity and an early expansion of *gsc* and *chd*. These data strongly suggest that Vrtn functions in parallel with the presently known maternal DV regulators. Indeed, our observations clearly indicate that Vrtn cooperates with β-catenin 2 in DV patterning. In the absence of Vrtn function, the embryo becomes extremely sensitive to ventralisation following reduction of vegetal DDs or β-catenin 2 activity. This could partially explain the mildly ventralised phenotype of MZ*vrtn* mutants, which may be also due to the induction of a possible compensatory mechanism, as observed in many genetic mutations (Rossi et al., 2015). It is noteworthy that the *ichabod* mutation that disrupts β-catenin 2 also displays a varied expressivity (Kelly et al., 2000), suggesting that a compensatory network may exist to protect DV patterning.

Both Vrtn overexpression and VAb@2cell similarly inhibit *bmp2b* marginal transcription at shield stage, and restrict its

expression in I-YSL during gastrulation. This situation is highly similar to that in MZ*smad5* mutants (Hild et al., 1999; Kondo, 2007), and further supports the hypothesis that Vrtn functions specifically to regulate BMP signalling. However, unlike MZ*smad5* mutants, cells from VAb@2cell embryos are capable of interpreting BMP signal, suggesting that Vrtn is not a component of the BMP pathway, but it functions as a regulator for *bmp2b* transcription. Our data confirm that Vrtn is a nuclear protein both in zebrafish and mammalian cells, as previously reported (Mikawa et al., 2011). Although it does not contain classical NLS, there is a possibility that the protein may be recognised by the non-classical nuclear import pathway (Soniat and Chook, 2015). Most importantly, both ChIP and EMSA strongly indicate that Vrtn directly binds a 59 bp sequence upstream of *bmp2b* transcription start site where no Smad-binding motif can be predicted. Thus, it is likely that Vrtn represses Smad5-mediated *bmp2b* transcription at the margin by binding to distinct DNA motifs. Further studies are needed to test this possibility.

It should be mentioned that Vrtn alone would not be sufficient to account for the VAb@2cell-induced dorsalisation. In particular, how does the repressor function of Vrtn become activated in VAb@2cell embryos? Why do *vrtn* mutants display a mildly ventralised phenotype? Are Vrtn antagonists removed after VAb@2cell? Although these questions are still open to further investigation, one likely explanation may be presence of other vegetally localised putative Vrtn antagonists, which are involved in the activation or 'de-repression' of BMP signalling in the margin and ventral ectoderm during gastrula stages. These factors may move relatively slowly after fertilisation, and their transport would persist during early cleavage stages. Supporting this hypothesis, we find that vegetal RNAs from the 2- to 4-cell stages, but not from later stages, possess an activity to antagonise the dorsalising effect of Vrtn. Further study will be necessary to formally identify these antagonists and to elucidate their mode of interaction with Vrtn in DV patterning. Taking all these aspects into consideration, we propose a 'dual-factor' model to explain how Vrtn functions in DV patterning (Fig. 9). Vrtn normally acts as a *bmp2b* repressor, and competes with its antagonists, either directly or indirectly, to regulate zygotic *bmp2b* transcription for the establishment of a BMP signalling gradient. In VAb@1cell embryos, all vegetal factors are removed, including DDs, Vrtn and Vrtn antagonists. In the absence of inhibition, *bmp2b* expression is enhanced and the embryos are ventralised. By contrast, in VAb@2cell embryos, most of the Vrtn antagonists and part of DDs are removed, but sufficient amounts of Vrtn are transported to the blastoderm, and are freed from its antagonists. This leads to inhibition of BMP signalling and dorsalisation, even though the activity of DDs may be reduced. In accordance with this hypothesis, VAb@2cell is unable to dorsalise MZ*vrtn* embryos due to the absence of Vrtn. In this situation, the ablated MZ*vrtn* embryos only maintain a reduced amount of DDs, similar to VAb@1cell in wild-type embryos. Thus, it is not surprising that VAb@2cell MZ*vrtn* embryos exhibit an increased *bmp2b* expression and a severely ventralised phenotype.

In conclusion, Vrtn is novel maternal transcriptional repressor that modulates zygotic *bmp2b* expression to maintain a correct BMP gradient along the DV axis. It acts independently of the dorsal organiser to prevent an excess of ventral fate in the early embryo. To further decipher the mechanism by which it regulates DV patterning, it will be interesting to identify potential Vrtn-associated events such as the presence and activity of Vrtn-antagonising factors and interacting proteins.
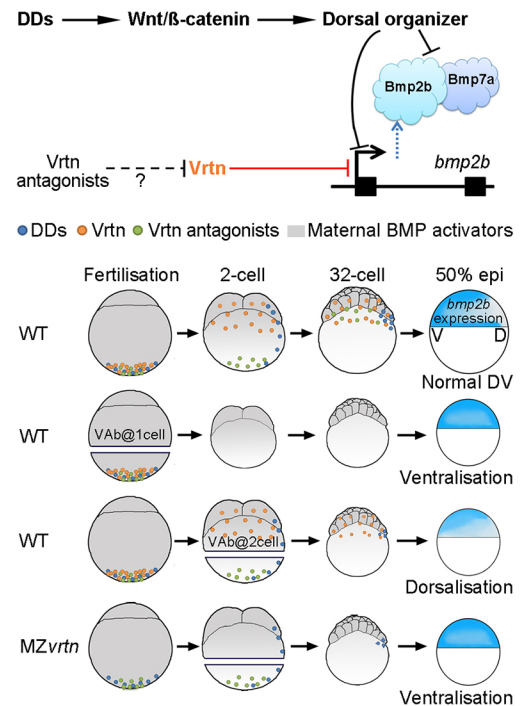

Fig. 9. The 'dual-factor' model. Vrtn and its putative antagonists are vegetally localised factors that function independently of DDs. Vrtn is translocated quickly towards the animal pole to inhibit *bmp2b* marginal transcription, whereas its antagonists are translocated relatively slowly, and should activate BMP signalling. VAb@1cell enhances *bmp2b* expression and ventralisation by removing both Vrtn and DDs. VAb@2cell, however, results in deficient *bmp2b* transcription and dorsalisation by removing Vrtn antagonists. In MZ*vrtn* embryos subjected to VAb@2cell, the absence of Vrtn and partial loss of DDs enhance *bmp2b* expression and produce ventralisation. It is clear that the dorsal fate is induced by maternal DDs and is protected by repression of both maternal and zygotic ventralising signals.

MATERIALS AND METHODS
Zebrafish
Zebrafish AB and TU strains were maintained at 28.5°C in the laboratory, and synchronously fertilised eggs were obtained as described previously (Shao et al., 2012). The animal experiments were approved by the Animal Ethics Committee of Shandong University, China and were performed according to their guidelines.

VAb
Fertilised eggs were dechorionated and transferred to an agar-coated Petri dish containing 1/3×Ringer's supplemented with 1.6% egg albumen and penicillin-streptomycin. The vegetal-most region of the yolk cell was punched using a sharp steel needle, and one half of the vegetal-most yolk cell content was then removed by cutting the equator of the yolk cell using a triangle-looped stainless steel wire (Movie 2). To synchronise the VAb under different experimental conditions, five embryos from each group were subjected to microsurgery in an alternating manner. After wound healing, the chorion-free embryos were cultured in a glass Petri dish with fresh culture medium to appropriate stages.

Immunofluorescence and western blotting
For immunofluorescence, the embryos were fixed overnight with 4% paraformaldehyde at 4°C and long-term stored in methanol at −20°C. They were treated with 0.15 M Tris-HCl (pH 9.0) at 70°C for 15 min, and washed three times in phosphate-buffered saline with Tween-20 (PBST), followed by incubation at 4°C overnight with anti-β-catenin antibody (1:500, Abcam, ab6302), anti-myc antibody (1:500, Santa Cruz Biotechnology, 9E10), or anti-P-Smad1/5/8 antibody (1:200, Cell Signaling, 9511L). The embryos

were washed several times in PBST and incubated with Alexa-488-conjugated secondary antibody (1:1000, Interchim) for 1 h at room temperature. After washing three times in PBST, they were counterstained with DAPI and mounted in 1% low-melting agarose. When necessary, the yolk was manually removed and the explants were cleared in ClearSee solution (Kurihara et al., 2015). The animal pole region was placed towards the objective lens of a confocal microscope (Zeiss, LSM700) and scanned several optical sections around the margin.

Western blotting was performed as described previously (Qi et al., 2017). The samples were probed with P-Smad1/5/8 antibody (1/1000) and β-actin antibody (1:5000, Proteintech, 66009-1-Ig) was used as a loading control. The protein bands were quantified using Lane 1D software (Sagecreation).

Transplantation
The embryos were injected with RLDx and labelled cells from the animal pole region at sphere stage were transplanted to the margin of unlabelled recipients in Ringer's without egg albumen. Chimeric embryos were cultured in 1/3×Ringer's with 1.6% egg albumen and antibiotics, and fixed at appropriate stages with 4% paraformaldehyde overnight at room temperature. For transplantation of mixed cells, synchronously fertilised eggs were labelled with FLDx or RLDx. At sphere stage, 20 blastoderms from labelled embryos were treated with trypsin-EDTA solution (2 mg/ml trypsin, 1 mM EDTA in PBS) at 37°C for 15 min, and dissociated into single cells by gentle pipetting. FLDx- and RLDx-labelled cells were thoroughly mixed and collected by centrifugation at 250 *g*. The cell pellet was suspended in Ringer's and a small fraction of mixed cells was microinjected into the ventral margin of unlabelled wild-type recipients at shield stage.

Extraction and injection of vegetal RNAs
MZ*vrtn* embryos were dechorionated and the animal halves were removed. The remaining vegetal explants were immediately transferred to Trizol reagent (Invitrogen). For each stage, total RNAs from 50 vegetal explants were dissolved in 3 μl RNase-free water. An equal volume of synthetic *vrtn* mRNA (100 ng/μl) and the vegetal RNAs were thoroughly mixed, and a mixture (5 nl) was injected into each embryo.

RNA-seq
Total RNAs were isolated from animal and vegetal pole regions dissected at the one-cell stage. The mRNA libraries were constructed using the TruSeq RNA Library Preparation Kit and 100 bp paired end sequencing was performed on Illumina HiSeq 2000. RNA-Seq data were aligned to reference transcriptome assembly (www.ensembl.org) and analysed using EdgeR software.

CRISPR/Cas9-mediated genome editing
The zebrafish codon-optimised Cas9 cDNA (Liu et al., 2014) was linearised with XbaI for synthesis of capped mRNA using mMESSAGE mMACHINE T7 kit. The *vrtn* targeting sequence was cloned into p-T7-gRNA vector, and the DNA template for *in vitro* transcription of target-specific gRNA was PCR-amplified as described (Xiao et al., 2013). Synthetic *Cas9* mRNA (200 pg) and gRNA (200 pg) were co-injected into one-cell stage embryos. The targeting efficiency was determined by sequencing PCR fragment amplified from genomic DNA extracted from a pool of 10 randomly selected embryos at 24 hpf using genotyping primers (Table S2). When mutated sequences were detected, the remaining embryos were raised to adulthood. These F0 fish were outcrossed with wild-type fish, and heterozygote F1 fish were screened using genomic DNA extracted from the tail fins. Homozygous mutants were obtained by intercrossing heterozygous carriers, and further confirmed by allele-specific PCR using primers listed in Table S2.

Morpholinos
The *bmp2b*MO (Lele et al., 2001), *vrtn*MO (5′-AATCAGTTCCGTAAAGTAGTCAGGT-3′), and *β-catenin2*MO (Bellipanni et al., 2006) were from Gene Tools and were suspended in sterile water.

In situ hybridisation and qRT-PCR
Antisense RNA probe labelling and *in situ* hybridisation were carried out as described previously (Shao et al., 2012). The probes for *dha/boz*, *gsc*, *chd*, *eve1*, *gata2a*, *ntla* and *dystrophin* have been described previously (Cao et al., 2012, 2014). Other probes were PCR amplified and cloned in the pGEM-T vector (Promega). For qRT-PCR, total RNAs were extracted from a pool of 20 embryos using Trizol reagent and treated with DNase I. They were reverse transcribed using M-MLV reverse transcriptase (Invitrogen), and qPCR with specific primers (Table S2) was performed using Quant qRT-PCR kit (Tiangen). The $2^{-\Delta\Delta Ct}$ method was employed to estimate the relative expression level.

Constructs and luciferase assays
The coding regions of zebrafish *bmp2b*, *vrtn*, *dazl*, *celf1* and *magoh* were cloned in pCS2 vector to generate untagged constructs. C-terminally GFP- or myc-tagged full-length and truncated Vrtn proteins, and RFP-tagged Histone2B were also cloned in pCS2 vector.

For the one-hybrid assay, the full-length and truncated Vrtn, the VP16 activation domain, and the *Drosophila* engrailed repressor domain (Li et al., 2006) were fused with the Gal4 DNA-binding domain at its C-terminal region and cloned in the pCS2 vector. To generate reporter constructs, the CMV promoter in the pCS2 vector harbouring the luciferase sequence was substituted for by 5 *UAS* elements and an *hsp70* minimal promoter to construct the *5×UAS-hsp-luc* reporter gene. The control reporter *xbra-luc* has been described previously (Cao et al., 2012). Synthetic mRNA (100 pg) corresponding to different fusion proteins was co-injected with the reporter DNA (50 pg) at the one-cell stage, and 15 embryos at 70% epiboly were lysed for luciferase assays using the Dual-Luciferase Reporter Assay System (Promega). The value in the control condition was set as 1, and expressed as relative luciferase activity (RLU).

For the assay of the Vrtn-responsive *bmp2b* regulatory region, the *bmp2b* −5701 to −3772 sequence and the −800 to +605 region relative to the *bmp2b* transcription start site were fused to the luciferase reporter, and cloned in pCS2 vector. The embryos were injected with the reporter DNA (20 pg) alone or co-injected with *vrtn*-myc mRNA, and were collected at 50% epiboly for luciferase assay as above.

Cell transfection
The expression vectors Vrtn-GFP and Histone2B-RFP were co-transfected in COS7 cells using the jetPRIME Transfection Reagent (Polyplus, PT-114-15) as described previously (Liu et al., 2017). The cells were examined and imaged 2 days after transfection.

Time-lapse imaging
Donor embryos were co-injected with synthetic mRNAs coding for Vrtn-GFP and Histone2B-RFP at the one-cell stage. At sphere stage, a small group of cells from the animal pole region were aspirated with a microinjection needle and injected into the corresponding region of uninjected recipients. At 50% epiboly, chimeric embryos were embedded in 1.5% low-melting agarose in a 12-well plate, and live images were recorded under a 20× objective using a High Content Live-Cell Imaging System (ImageXpress Micro-4, MD). Time-lapse movies were generated using ImageJ software (NIH Image).

ChIP and EMSA
For ChIP, synthetic *vrtn*-myc mRNA was injected at the one-cell stage, and 230 injected embryos at 50% epiboly were crosslinked with 4% paraformaldehyde in 200 mM phosphate buffer. The chromatins were sonicated for 20 s at 200 W four times at one minute intervals. They were precipitated using 1 μg anti-myc antibody (Santa Cruz Biotechnology, 9E10) or an equal amount of unrelated IgG (Abcam, ab18413) as a control. The *bmp2b* regulatory region was analysed by semi-quantitative PCR or by qPCR in triplicate using the primers listed in Table S2.

For EMSAs, synthetic *vrtn-myc* mRNA was injected at the one-cell stage, and nuclear extracts from 150 injected or uninjected embryos at shield stage were prepared using the NE-PER Nuclear and Cytoplasmic Extraction Reagents (Thermo Scientific, 78833). Single-strand oligonucleotide probes were labelled using the Biotin 3′ End DNA Labelling Kit (Thermo Scientific, 89818), and were annealed to generate double-stranded DNA probes (Table S3). EMSAs were performed following the recommendation in the LightShift EMSA Optimization & Control Kit (Thermo Scientific, 20148X).

Data availability

The RNA-seq data supporting this work are available from Gene Expression Omnibus with accession number GSE103090.

Supplementary information

Supplementary information available online at
http://dev.biologists.org/lookup/doi/10.1242/dev.152553.supplemental

References

Abrams, E. W. and Mullins, M. C. (2009). Early zebrafish development: it's in the maternal genes. *Curr. Opin. Genet. Dev.* **19**, 396-403.

Bellipanni, G., Varga, M., Maegawa, S., Imai, Y., Kelly, C., Myers, A. P., Chu, F., Talbot, W. S. and Weinberg, E. S. (2006). Essential and opposing roles of zebrafish beta-catenins in the formation of dorsal axial structures and neurectoderm. *Development* **133**, 1299-1309.

Cao, J.-M., Li, S.-Q., Zhang, H.-W. and Shi, D.-L. (2012). High mobility group B proteins regulate mesoderm formation and dorsoventral patterning during zebrafish and Xenopus early development. *Mech. Dev.* **129**, 263-274.

Cao, J., Li, S., Shao, M., Cheng, X., Xu, Z. and Shi, D. (2014). The PDZ-containing unconventional myosin XVIIIA regulates embryonic muscle integrity in zebrafish. *J. Genet. Genomics* **41**, 417-428.

Carron, C. and Shi, D.-L. (2016). Specification of anteroposterior axis by combinatorial signaling during Xenopus development. *Wiley Interdiscip. Rev. Dev. Biol.* **5**, 150-168.

Cuykendall, T. N. and Houston, D. W. (2009). Vegetally localized Xenopus trim36 regulates cortical rotation and dorsal axis formation. *Development* **136**, 3057-3065.

De Robertis, E. M. (2006). Spemann's organizer and self-regulation in amphibian embryos. *Nat. Rev. Mol. Cell Biol.* **7**, 296-302.

Dick, A., Hild, M., Bauer, H., Imai, Y., Maifeld, H., Schier, A. F., Talbot, W. S., Bouwmeester, T. and Hammerschmidt, M. (2000). Essential role of Bmp7 (snailhouse) and its prodomain in dorsoventral patterning of the zebrafish embryo. *Development* **127**, 343-354.

Dosch, R. and Niehrs, C. (2000). Requirement for anti-dorsalizing morphogenetic protein in organizer patterning. *Mech. Dev.* **90**, 195-203.

Flores, M. V. C., Lam, E. Y. N., Crosier, K. E. and Crosier, P. S. (2008). Osteogenic transcription factor Runx2 is a maternal determinant of dorsoventral patterning in zebrafish. *Nat. Cell Biol.* **10**, 346-352.

Ge, X., Grotjahn, D., Welch, E., Lyman-Gingerich, J., Holguin, C., Dimitrova, E., Abrams, E. W., Gupta, T., Marlow, F. L., Yabe, T. et al. (2014). Hecate/Grip2a acts to reorganize the cytoskeleton in the symmetry-breaking event of embryonic axis induction. *PLoS Genet.* **10**, e1004422.

Goutel, C., Kishimoto, Y., Schulte-Merker, S. and Rosa, F. (2000). The ventralizing activity of Radar, a maternally expressed bone morphogenetic protein, reveals complex bone morphogenetic protein interactions controlling dorso-ventral patterning in zebrafish. *Mech. Dev.* **99**, 15-27.

Hild, M., Dick, A., Rauch, G. J., Meier, A., Bouwmeester, T., Haffter, P. and Hammerschmidt, M. (1999). The smad5 mutation somitabun blocks Bmp2b

signaling during early dorsoventral patterning of the zebrafish embryo. *Development* **126**, 2149-2159.

Inui, M., Montagner, M., Ben-Zvi, D., Martello, G., Soligo, S., Manfrin, A., Aragona, M., Enzo, E., Zacchigna, L., Zanconato, F. et al. (2012). Self-regulation of the head-inducing properties of the Spemann organizer. *Proc. Natl. Acad. Sci. USA* **109**, 15354-15359.

Jesuthasan, S. and Strähle, U. (1997). Dynamic microtubules and specification of the zebrafish embryonic axis. *Curr. Biol.* **7**, 31-42.

Kapp, L. D., Abrams, E. W., Marlow, F. L. and Mullins, M. C. (2013). The integrator complex subunit 6 (Ints6) confines the dorsal organizer in vertebrate embryogenesis. *PLoS Genet.* **9**, e1003822.

Kelly, C., Chin, A. J., Leatherman, J. L., Kozlowski, D. J. and Weinberg, E. S. (2000). Maternally controlled (beta)-catenin-mediated signaling is required for organizer formation in the zebrafish. *Development* **127**, 3899-3911.

Kishimoto, Y., Lee, K. H., Zon, L., Hammerschmidt, M. and Schulte-Merker, S. (1997). The molecular nature of zebrafish swirl: BMP2 function is essential during early dorsoventral patterning. *Development* **124**, 4457-4466.

Kondo, M. (2007). Bone morphogenetic proteins in the early development of zebrafish. *FEBS J.* **274**, 2960-2967.

Kurihara, D., Mizuta, Y., Sato, Y. and Higashiyama, T. (2015). ClearSee: a rapid optical clearing reagent for whole-plant fluorescence imaging. *Development* **142**, 4168-4179.

Langdon, Y. G. and Mullins, M. C. (2011). Maternal and zygotic control of zebrafish dorsoventral axial patterning. *Annu. Rev. Genet.* **45**, 357-377.

Langdon, Y. G., Fuentes, R., Zhang, H., Abrams, E. W., Marlow, F. L. and Mullins, M. C. (2016). Split top: a maternal cathepsin B that regulates dorsoventral patterning and morphogenesis. *Development* **143**, 1016-1028.

Lele, Z., Bakkers, J. and Hammerschmidt, M. (2001). Morpholino phenocopies of the swirl, snailhouse, somitabun, minifin, silberblick, and pipetail mutations. *Genesis* **30**, 190-194.

Leung, T., Bischof, J., Soll, I., Niessing, D., Zhang, D., Ma, J., Jackle, H. and Driever, W. (2003). bozozok directly represses bmp2b transcription and mediates the earliest dorsoventral asymmetry of bmp2b expression in zebrafish. *Development* **130**, 3639-3649.

Li, H.-Y., Bourdelas, A., Carron, C., Gomez, C., Boucaut, J.-C. and Shi, D.-L. (2006). FGF8, Wnt8 and Myf5 are target genes of Tbx6 during anteroposterior specification in Xenopus embryo. *Dev. Biol.* **290**, 470-481.

Little, S. C. and Mullins, M. C. (2009). Bone morphogenetic protein heterodimers assemble heteromeric type I receptor complexes to pattern the dorsoventral axis. *Nat. Cell Biol.* **11**, 637-643.

Liu, D., Wang, Z., Xiao, A., Zhang, Y., Li, W., Zu, Y., Yao, S., Lin, S. and Zhang, B. (2014). Efficient gene targeting in zebrafish mediated by a zebrafish-codon-optimized cas9 and evaluation of off-targeting effect. *J. Genet. Genomics* **41**, 43-46.

Liu, C., Zhai, X., Zhao, B., Wang, Y. and Xu, Z. (2017). Cyclin I-like (CCNI2) is a cyclin-dependent kinase 5 (CDK5) activator and is involved in cell cycle regulation. *Sci. Rep.* **7**, 40979.

Lu, F.-I., Thisse, C. and Thisse, B. (2011). Identification and mechanism of regulation of the zebrafish dorsal determinant. *Proc. Natl. Acad. Sci. USA* **108**, 15876-15880.

Maegawa, S., Yasuda, K. and Inoue, K. (1999). Maternal mRNA localization of zebrafish DAZ-like gene. *Mech. Dev.* **81**, 223-226.

Marlow, F. L. and Mullins, M. C. (2008). Bucky ball functions in Balbiani body assembly and animal-vegetal polarity in the oocyte and follicle cell layer in zebrafish. *Dev. Biol.* **321**, 40-50.

Mei, W., Lee, K. W., Marlow, F. L., Miller, A. L. and Mullins, M. C. (2009). hnRNP I is required to generate the Ca2+ signal that causes egg activation in zebrafish. *Development* **136**, 3007-3017.

Mikawa, S., Sato, S., Nii, M., Morozumi, T., Yoshioka, G., Imaeda, N., Yamaguchi, T., Hayashi, T. and Awata, T. (2011). Identification of a second gene associated with variation in vertebral number in domestic pigs. *BMC Genet.* **12**, 5.

Miller, J. R., Rowning, B. A., Larabell, C. A., Yang-Snyder, J. A., Bates, R. L. and Moon, R. T. (1999). Establishment of the dorsal-ventral axis in Xenopus embryos coincides with the dorsal enrichment of dishevelled that is dependent on cortical rotation. *J. Cell Biol.* **146**, 427-438.

Mizuno, T., Yamaha, E., Kuroiwa, A. and Takeda, H. (1999). Removal of vegetal yolk causes dorsal deficencies and impairs dorsal-inducing ability of the yolk cell in zebrafish. *Mech. Dev.* **81**, 51-63.

Nguyen, V. H., Schmid, B., Trout, J., Connors, S. A., Ekker, M. and Mullins, M. C. (1998). Ventral and lateral regions of the zebrafish gastrula, including the neural crest progenitors, are established by a bmp2b/swirl pathway of genes. *Dev. Biol.* **199**, 93-110.

Nojima, H., Rothhamel, S., Shimizu, T., Kim, C.-H., Yonemura, S., Marlow, F. L. and Hibi, M. (2010). Syntabulin, a motor protein linker, controls dorsal determination. *Development* **137**, 923-933.

Ober, E. A. and Schulte-Merker, S. (1999). Signals from the yolk cell induce mesoderm, neuroectoderm, the trunk organizer, and the notochord in zebrafish. *Dev. Biol.* **215**, 167-181.

DEVELOPMENT

Qi, J., Lee, H.-J., Saquet, A., Cheng, X.-N., Shao, M., Zheng, J. J. and Shi, D.-L. (2017). Autoinhibition of Dishevelled protein regulated by its extreme C terminus plays a distinct role in Wnt/β-catenin and Wnt/planar cell polarity (PCP) signaling pathways. *J. Biol. Chem.* **292**, 5898-5908.

Ramel, M.-C., Buckles, G. R., Baker, K. D. and Lekven, A. C. (2005). WNT8 and BMP2B co-regulate non-axial mesoderm patterning during zebrafish gastrulation. *Dev. Biol.* **287**, 237-248.

Reim, G. and Brand, M. (2006). Maternal control of vertebrate dorsoventral axis formation and epiboly by the POU domain protein Spg/Pou2/Oct4. *Development* **133**, 2757-2770.

Reversade, B., Kuroda, H., Lee, H., Mays, A. and De Robertis, E. M. (2005). Depletion of Bmp2, Bmp4, Bmp7 and Spemann organizer signals induces massive brain formation in Xenopus embryos. *Development* **132**, 3381-3392.

Ro, H. and Dawid, I. B. (2009). Organizer restriction through modulation of Bozozok stability by the E3 ubiquitin ligase Lnx-like. *Nat. Cell Biol.* **11**, 1121-1127.

Rossi, A., Kontarakis, Z., Gerri, C., Nolte, H., Hölper, S., Krüger, M. and Stainier, D. Y. R. (2015). Genetic compensation induced by deleterious mutations but not gene knockdowns. *Nature* **524**, 230-233.

Schmid, B., Fürthauer, M., Connors, S. A., Trout, J., Thisse, B., Thisse, C. and Mullins, M. C. (2000). Equivalent genetic roles for bmp7/snailhouse and bmp2b/swirl in dorsoventral pattern formation. *Development* **127**, 957-967.

Shao, M., Lin, Y., Liu, Z., Zhang, Y., Wang, L., Liu, C. and Zhang, H. (2012). GSK-3 activity is critical for the orientation of the cortical microtubules and the dorsoventral axis determination in zebrafish embryos. *PLoS ONE* **7**, e36655.

Sidi, S., Goutel, C., Peyriéras, N. and Rosa, F. M. (2003). Maternal induction of ventral fate by zebrafish radar. *Proc. Natl. Acad. Sci. USA* **100**, 3315-3320.

Slack, J. (2014). Establishment of spatial pattern. *Wiley Interdiscip. Rev. Dev. Biol.* **3**, 379-388.

Soniat, M. and Chook, Y. M. (2015). Nuclear localization signals for four distinct karyopherin-β nuclear import systems. *Biochem. J.* **468**, 353-362.

Stickney, H. L., Imai, Y., Draper, B., Moens, C. and Talbot, W. S. (2007). Zebrafish bmp4 functions during late gastrulation to specify ventroposterior cell fates. *Dev. Biol.* **310**, 71-84.

Sun, Y., Tseng, W.-C., Fan, X., Ball, R. and Dougan, S. T. (2014). Extraembryonic signals under the control of MGA, Max, and Smad4 are required for dorsoventral patterning. *Dev. Cell* **28**, 322-334.

Suzuki, H., Maegawa, S., Nishibu, T., Sugiyama, T., Yasuda, K. and Inoue, K. (2000). Vegetal localization of the maternal mRNA encoding an EDEN-BP/Bruno-like protein in zebrafish. *Mech. Dev.* **93**, 205-209.

Tao, Q., Yokota, C., Puck, H., Kofron, M., Birsoy, B., Yan, D., Asashima, M., Wylie, C. C., Lin, X. and Heasman, J. (2005). Maternal wnt11 activates the canonical wnt signaling pathway required for axis formation in Xenopus embryos. *Cell* **120**, 857-871.

Tran, L. D., Hino, H., Quach, H., Lim, S., Shindo, A., Mimori-Kiyosue, Y., Mione, M., Ueno, N., Winkler, C., Hibi, M. et al. (2012). Dynamic microtubules at the vegetal cortex predict the embryonic axis in zebrafish. *Development* **139**, 3644-3652.

Weaver, C., Farr, G. H., Pan, W., Rowning, B. A., Wang, J., Mao, J., Wu, D., Li, L., Larabell, C. A. and Kimelman, D. (2003). GBP binds kinesin light chain and translocates during cortical rotation in Xenopus eggs. *Development* **130**, 5425-5436.

Xiao, A., Wang, Z., Hu, Y., Wu, Y., Luo, Z., Yang, Z., Zu, Y., Li, W., Huang, P., Tong, X. et al. (2013). Chromosomal deletions and inversions mediated by TALENs and CRISPR/Cas in zebrafish. *Nucleic Acids Res.* **41**, e141.

Xue, Y., Zheng, X., Huang, L., Xu, P., Ma, Y., Min, Z., Tao, Q., Tao, Y. and Meng, A. (2014). Organizer-derived Bmp2 is required for the formation of a correct Bmp activity gradient during embryonic development. *Nat. Commun.* **5**, 3766.

DEVELOPMENT